The first adaptive optics closed loop imaging demonstration of a large segmented telescope with a space-borne laser guide star

Eliad Peretz[*a], Peter Wizinowich[b], Eduardo Marin[b], Richard Butler[a], Kevin Hall[a], Lucas Pabarcius[a], Susana Deustua[a,d], Maxwell A. Millar-Blanchaer[c], Bert Pasquale[a], John Mather[a], Keshet Shavit[a,d], Richard Slonaker[a], Jean-Pierre Chamoun[a], Nick Cummings[a], Andrew DeAbreu[a], David Hahn[a], Lori Jones[a], Karen Keadle-Calvert[a], Dutch Lamberson[a], Matt McGinnis[a], Greg Menke[a], Bill Muscovich[a], Tim Singletary[a], Mark Sinkiat[a], John Smith[a], Kenny Sterling[a], Miriam Wennersten[a], Jonathon Woodward[a], Joshua Blair[a], Rick Blair[a], Frank Chavez[a], Jacob Cohn[a], Scott Crosier[a], Julian Hayes[a], Adam Isleib[a], Miguel Saenz[a], Scott Stephens[a], Jose Talamantes[a], Robert Lafon[a], Carlos Alverez[b], Antonin Bouchez[b], Jason Chin[b], Jacques-Robert Delorme[b], Charlotte Guthery[b], Luke Gers[b], Shui Hung Kwok[b], Scott Lilley[b], Jim Lyke[b], Rosalie McGurk[b], Marc Kassis[b], John O'Meara[b], John Pelletier[b], Brett Smith[b], Max Service[b], Matt Wahl[b], Ed Wetherell[b], Sam Ragland[b], Rebecca Jensen-Clem[e], Peter Kurczynski-[a], Eric L. Nielsen[i], Imke de Pater[g], Greg Aldering[j], Peter Plavchan[f], Kayla Carmical[a], Ariel Horesh[a], Jonathan Horesh[a], Andrew Lewis[a], Joseph Schlager[a], Sara Seager[j,k,l]

[a]NASA Goddard Space Flight Center, Greenbelt, MD 20771, USA
[b]W. M. Keck Observatory, Kamuela, HI 96743, USA
[c]University of California Santa Barbara, CA 91125, USA
[d]National Institute of Standards and Technology, Gaithersburg, MD 20899, USA
[e]University of California, Santa Cruz, Santa Cruz, CA 95064, USA
[f]George Mason University, Fairfax, Virginia 22030, USA
[g]University of California, Berkeley, Berkeley, CA, USA
[j]Lawrence Berkeley National Lab, Berkeley, CA, 94720. USA
[h]University of California Irvine, Irvine, CA 92697, USA-
[i]New Mexico State University, Las Cruces, NM 88003, USA
[j]Massachusetts Institute of Technology, Cambridge, MA 01742, USA

Abstract. The Orbiting Configurable Artificial Star (ORCAS) mission, in collaboration with the W. M. Keck Observatory (WMKO) and the Laser Communication Relay Demonstration (LCRD), conducted an on-sky experiment aimed at advancing the ORCAS mission concept maturity level (CML) and technology readiness level (TRL) in preparation for a full mission proposal. The experimental goals span across technical, programmatic, and scientific domains; Ultimately demonstrating for the first time adaptive optics (AO) closed loop imaging of a large segmented telescope with a space-borne laser guide star, testing hybrid observatories' operational methodology and robustness, and provided valuable insights for future flux calibration testing of space-borne laser systems (including post-processing).

Keywords: ORCAS, W. M. Keck Observatory, LCRD, Adaptive Optics, Artificial Orbiting Guide Star, Hybrid Observatories.

*Eliad Peretz, eliad.peretz@gmail.com

1 Introduction

Over the past two decades, ground-based observatories have achieved transformative gains in angular resolution and image quality through the development of advanced adaptive optics (AO) systems. However, despite these advances, AO performance at visible wavelengths remains limited by the brightness and proximity of natural guide stars, as well as by the finite power and range of conventional ground-based laser guide stars (LGS). These constraints have motivated a new class of hybrid observatories, in which a space-borne laser beacon provides a stable, high-altitude wavefront reference for large ground-based telescopes. Such architectures offer a pathway to extend AO correction into shorter wavelengths, improve flux calibration precision, and enable unique operational modes that combine the strengths of both space and ground platforms.

Hybrid observatories typically consist of a space segment, such as an orbiting laser beacon or payload, and a ground segment consisting of one or more large telescopes. By leveraging the large apertures, flexible instrumentation, and servicing capabilities of ground facilities, while simultaneously exploiting the stability and high vantage point of space-borne sources, hybrid systems can deliver diffraction-limited performance at visible wavelengths at substantially lower cost than comparable space telescopes. Over the past several years, multiple hybrid mission concepts have emerged including ORCAS, QUSAR, STAR-Lite, Landolt, and CANDLE, etc. reflecting a growing recognition of the scientific and technical opportunities afforded by this approach.

The ORCAS (Orbiting Configurable Artificial Star) mission concept, initiated in 2019, has played a central role in advancing the maturity of hybrid observatory architectures. ORCAS envisions deploying a satellite equipped with a stable laser beacon to act as an artificial guide star for large segmented telescopes such as Keck. By closing the AO loop on a spacecraft-borne source, ORCAS seeks to demonstrate high-resolution imaging at visible wavelengths, validate new operational models for coordinated ground–space observations, and enable precision flux calibration using a known reference above the atmosphere. In support of this concept, a series of precursor technology maturation activities, laboratory demonstrations, and mission design studies have been conducted over the past several years.

In early 2024, the ORCAS team, in collaboration with the W. M. Keck Observatory and NASA's Laser Communications Relay Demonstration (LCRD), conducted the first on-sky experiment to test these principles. The demonstration aimed to mature the Concept Maturity Level (CML) and Technology Readiness Level (TRL) of hybrid observatory operations by using Keck to lock onto and close the AO loop on a laser beacon aboard the geosynchronous LCRD payload. The experiment pursued four primary objectives: (1) to validate the operational model for hybrid observations, (2) to predict and track the trajectory of a spacecraft with sufficient accuracy to enable high-resolution observations, (3) to perform closed-loop AO imaging on a space-borne laser beacon, and (4) to explore the feasibility of flux calibration from a known power source in orbit. This represented the first adaptive optics closed-loop imaging demonstration of a large segmented telescope using a laser guide star in space.

The structure of this paper is as follows. In Section 1.1, we review recent developments in hybrid observation concepts and technologies, situating the ORCAS–Keck–LCRD experiment within a broader international context. Section 2 describes the generalized operational model for hybrid observatories and how it was applied using the LCRD payload. In Section 3, we present the trajectory prediction and tracking tools developed for the experiment. Section 4 discusses the

closed-loop AO imaging results, while Section 5 outlines lessons learned for future flux calibration missions such as Landolt. We conclude in Section 6 with a discussion of the implications of these results for future hybrid observatories and space–ground astronomical systems.

1.1 Recent Developments in Hybrid Observation

The concept of hybrid observatories and specifically linking space-borne laser beacons with large ground-based telescopes has gained increasing traction over the past decade as a practical pathway to achieve diffraction-limited imaging and precision flux calibration without relying solely on costly space telescopes. In this framework, the **Orbiting Configurable Artificial Star (ORCAS)** concept has played a foundational role. Initiated in **2019**, ORCAS proposed to place a satellite carrying a stable laser beacon in Earth orbit to serve as an artificial guide star for large segmented telescopes on the ground, such as Keck. The goal was to extend adaptive optics (AO) correction into the visible regime, develop operational models for joint space–ground observations, and enable flux calibration using a well-characterized source above the atmosphere. Over subsequent years, this concept has matured considerably, culminating in the 2024 Keck–LCRD demonstration described in this work, which constitutes the first closed-loop AO imaging of a spacecraft-borne laser beacon with a large segmented ground-based telescope.

This recent progress led to the development of a broader international landscape for hybrid mission concepts. In 2020, Di Rico and collaborators in Italy proposed the GO-ON mission, designed to pair the Large Binocular Telescope (LBT) in Arizona with a 6U CubeSat placed in a high elliptical orbit. The CubeSat would use a laser emission optical system operating between 600 nm and 1000 nm, effectively creating an artificial guide star in the visible and near-infrared. This approach aimed to achieve image quality up to an order of magnitude better than Hubble, but the project did not advance beyond the proposal stage.

In parallel, efforts in the United States focused on demonstrating key enabling technologies for hybrid systems. In May 2022, MIT Lincoln Laboratory launched the Agile Microsat (AMS), which carried the Beacon payload, a compact 0.5U laser terminal intended to validate CubeSat-based laser pointing and wavefront sensing. Through a sequence of tests conducted between June and September 2022, the AMS Beacon demonstrated stable pointing using a scanning pattern and achieved 2 kHz optical wavefront measurements from orbit, establishing CubeSats as viable low-cost platforms for artificial guide stars.

Significant advances have also taken place in the field of long-baseline optical interferometry (LBOI). Between 2022 and 2024, Glen Herriot and collaborators proposed and bench-tested a novel interferometric architecture that uses integrated photonics combined with a digitally modulated satellite beacon. Unlike traditional mechanical AO systems, this approach employs low-cost phase compensators operating at tens of kilohertz, providing a common phase reference across widely separated telescopes. Such a system aims to enable phase-aligned, micro-arcsecond resolution interferometry on a scale not previously achievable from the ground.

More recently, in 2024, Johnson et al. proposed STARLITE (Superluminous Tomographic Atmospheric Reconstruction with Laser-beacons for Imaging Terrestrial Exoplanets), a constellation of five 12U satellites placed in high elliptical orbits with apogees of approximately 350,000 km. Each satellite would host a 1 W laser at 750 nm, equivalent to a -10 mag source, to provide tomographic atmospheric reconstruction for ground-based observatories. The project is aimed at enabling sensitive detection of molecular oxygen in exoplanet atmospheres through high-resolution spectroscopy supported by space-based laser beacons.

In parallel with these technology demonstrations, NASA has recently initiated the **Landolt** mission, which represents a significant scientific application of the hybrid observatory framework.

Landolt is designed to place a laser beacon in a stable geosynchronous-like orbit, enabling precise flux calibration of ground-based telescopes by providing a well-characterized, stable optical source above the atmosphere. By observing this beacon simultaneously with celestial calibration targets, Landolt aims to reduce systematic uncertainties in photometric calibration to the millimagnitude level, a critical requirement for next-generation cosmology and time-domain surveys. Operationally, Landolt will employ a similar ground–space coordination model to that developed under ORCAS, validating both the technical approach and the mission concept maturity. Its implementation marks the transition of hybrid observatories from experimental demonstrations toward operational missions with direct scientific return.

Taken together, these developments illustrate the rapid evolution of hybrid observatory concepts with artificial light sources, since 2019. ORCAS has provided the operational and scientific backbone for this emerging class of missions, while complementary efforts in Europe and North America have demonstrated the enabling technologies from CubeSat laser pointing to photonic interferometry and constellation architectures that together point toward a new era of integrated space–ground astronomical systems.

1.2 Experiment Goals and Objectives

The ORCAS-Keck-LCRD experiment overarching goal is to advance the CML and TRL of hybrid observatories. To achieve that we identified key technical, programmatic and scientific goals as can be seen in Table 1 - To demonstrate hybrid observations can be performed.

Table 1: Experimental Goals and Requirements

Prefix	**Goal**	**Requirement**
1-3.T	Technical Goals	meets
1.T	Validate Mission Operational Model	Conduct AO/Flux observations
2.T	Predict and Measure Spacecraft Trajectory	Telemetry and Observational Data
3.T	Closed Loop AO Imaging	Pyramid Wavefront Sensor and NIRC2 Imager
1-3.P	Programmatic Goals	meets
1.P	Advance Operations TRL	Achieve goal 1.T
2.P	Advance Multi-observatory Applicability	Observe with at least two observatories
3.P	Mitigate Safety/other Concerns	Conduct Observation
1-2.S	Scientific Goals	meets
1.S	Flux Calibration	Imaging data of laser source and background stars
2.S	Science 2	Acquire images

The technical goals for this experiment are: (1) AO high-resolution imaging with a spacecraft carrying a laser beacon. (2) Operational rehearsals for hybrid observatories. (3) Flux calibration of standard stars using space-borne laser sources of known brightness, including post-processing.

(1) AO imaging of the LCRD laser: Requires closing the AO loop with the near-infrared pyramid wavefront sensor (PyWFS; Bond et al. 2020) on the LCRD laser source. Then demonstrate that the image of the laser source is near-diffraction limited on an imaging camera. The goal is to show the AO loop can be closed on a spacecraft's laser pointing toward the ground-based telescope.

(2) Validate operational model: Test, validate and update the operational modes of the ORCAS/CANDLE/Landolt Mission. This requires coordination of the space (LCRD) and ground (Keck) efforts for a successful observation. This will inform operational decisions, sequence of operations and other aspects that consider the Earth-Space system when designing the ORCAS mission.

(3) Flux calibration: Measure flux from the laser terminal and compare to background stars. This is done by recording images and/or spectra of the LCRD source and several standard stars on a detector. Observation of calibrated laser beam from Keck/and other ground-based telescopes. The calibrated laser beam will path through the earth's atmosphere, telescope and instrument (for example wavefront corrections) in the same way as the target stars - and this will reduce the flux calibration uncertainty.

All the technical goals above (1)-(3) in this experiment are a first step in achieving an hybrid observation and to show that the Keck telescope can operate with a NASA spacecraft to achieve and mature the hybrid observation missions. The telescope should collect/detect the laser source, and if possible from various ground sites - to demonstrate this could happen using telescopes at multiple locations.

2 Establishing an Operational Model for Hybrid Observatories

Hybrid Observatories are set to advance multiple scientific domains. From the ORCAS mission, which aims to achieve unprecedented high-resolution AO imaging at visible wavelengths, to the BHEX mission focusing on accessing the photon ring from strongly lensed photons at radio frequencies. Furthermore, these mission concepts hold the potential to substantially enhance flux calibration by measuring a known source in an Earth-bound orbit, a pioneering endeavor that the recently funded NASA's Landolt mission will undertake. Despite the diverse scientific objectives of these missions, they all share an array of common challenges. In this section we zoom in on how to effectively integrate space-based assets with ground-based facilities. In section 2.1, we propose a standardized operational procedure for future Hybrid Observatories that forthcoming missions can adopt. Finally, we discuss how we utilized the LCRD spacecraft to simulate a hybrid observation in section 2.2, demonstrating the practical application of our proposed model for the ORCAS mission.

2.1 Generalized Hybrid Operational Model

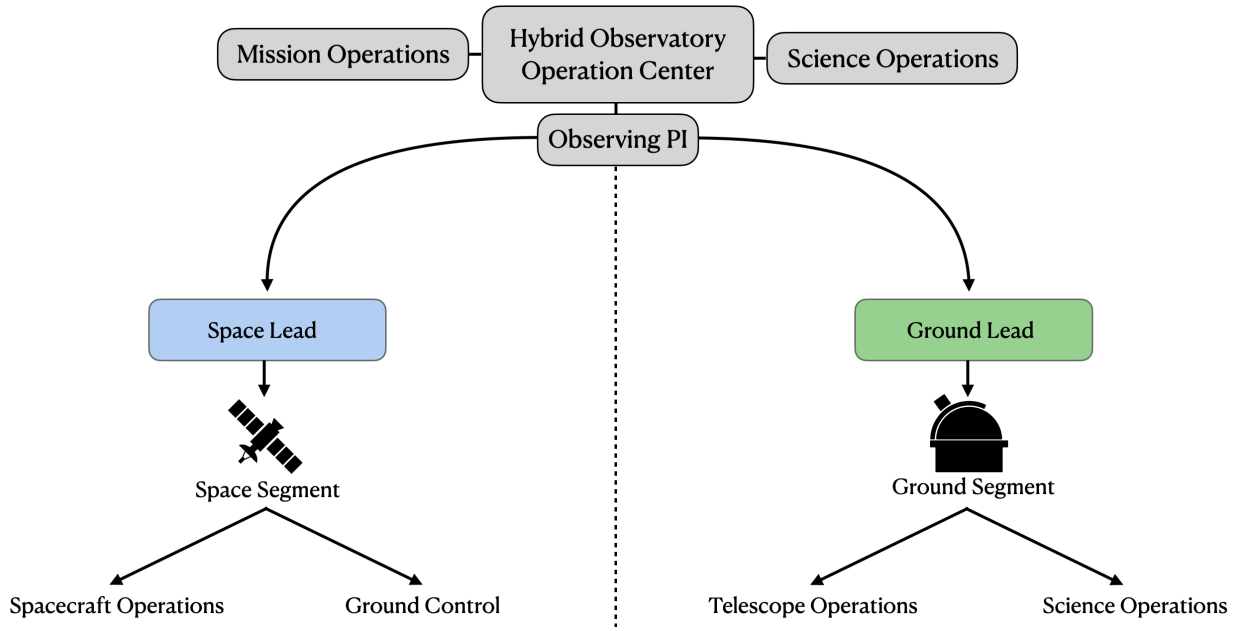

Fig 1: A flow chart of the Operational Model for Hybrid Observatories. The Space and Ground segments are independent components, each divided into two parts. Both will have a primary point of contact that will be in direct communication with the PI of the observation. Data from both the spacecraft and ground facilities will be transferred to the Mission Science Center, which operates as the nerve center of the hybrid observation.

Figure 1 presents a general flow chart of a hybrid observation. We begin with the Hybrid Observatory Operations Center: the nerve center of the hybrid observation. To be specific, the operations center does not require a specific location. The only requirement is that the Observing PI is present, as they are critical for a successful observation. The Observing PI will be in direct communication with the two segments: Space and Ground. Let's first consider the space segment, which refers to the spacecraft that will be working with the ground facility. The space segment

can be broken into two primary parts: (1) The spacecraft itself, and (2) the team at the control center operating the spacecraft. To achieve the science objectives of future hybrid observations, the spacecraft will need to perform a sequence of operations. These include station keeping, attitude control, telemetry, and any science payload operations. These operations will be performed by the spacecraft control team operating from their own ground station. The Space Segment Lead will be responsible for communicating all commands to the control team and relaying all data from the spacecraft to the Observing PI. Let's now consider the ground segment. It is broken up into two components: the (1) observatory operations and (2) science deliverables are all under the control of the Ground Operations Lead. This would refer to either observatory staff, or someone with expertise using the facility. In some cases, the Observing PI may also serve as the Ground Operations Lead. Just like the space segment, they will directly communicate with the Observing PI during all stages of the hybrid observation. All data collected from the ground facilities will be transferred to the Science Operations Center, which could simply be a remote observing room connected with an observatory. It is critical that each segment of the Hybrid Observation tree maintain their established communication lines.

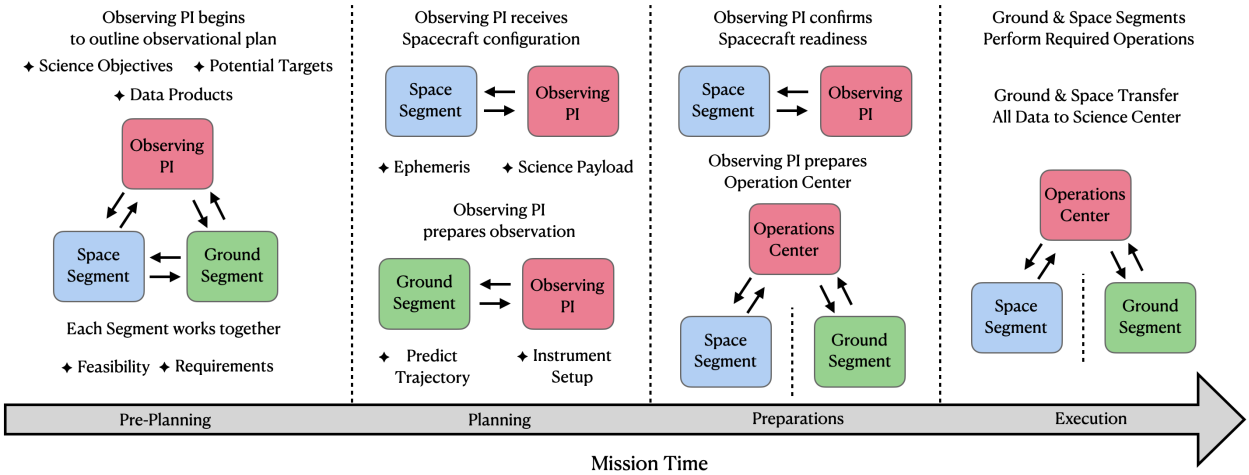

Fig 2: The different stages of a hybrid observation. We divide the total mission time into four segments: (1) Pre-Planning, (2) Planning, (3) Preparations, and (4) Execution. The time is not specified, as each Hybrid Observatory concept will require a unique timeline. It will be up to the Observing PI to properly allocate enough time for each stage to guarantee a successful observation.

Now that we have established the two segments of a hybrid observation, we transition into a generalized sequence of events. We stress that the specific operations of each upcoming mission will require special care to facilitate successful observations. Figure 2 provides a generalized timeline for the different stages required for Hybrid Observations. For each stage, we do not specify the amount of time that is required. To begin, a sequence of (1) Pre-Planning is required. Here, the Observing PI will communicate with both the ground and space segments to discuss the Science goals of the observation. The desired science will dictate how the hybrid observation will need to be executed and what will be needed from both the ground and space teams. We continue onto the (2) Planning stage. Now that the science objectives have been finalized, the ground and space segments focus their communication directly with the Observing PI. Specifically, the PI will make informed decisions on which instruments to use on the ground and decide on the final spacecraft configuration. It is critical that the communication follows the structure presented in

Figure 1 to avoid unnecessary disruption or confusion between the ground and space segments. This point is illustrated in Figure 2 by drawing mirrored arrows between the different segments. Next, we transition to the (3) Preparations stage. Here, the Observing PI will receive the final status of the spacecraft from the Space Lead, such as the spacecraft ephemeris, and relay it to the Ground Lead. At the same time, the PI will establish the operations center where they can maintain a direct line of communication between both the ground and space leads. Finally, we reach the (4) Execution stage. This simply refers to the phase where the Hybrid Observation is performed. All data, from both the spacecraft and ground facility, are transferred to the Operations Center. During the observation, the PI communicates with either the Ground or Space Lead if subsequent operations are required, such as altering instrument setup or deactivating a laser beacon. The key take-away from this generalized timeline is communication. Future Hybrid Observatories will only be as successful as the team managing and running them.

2.2 Simulating the Operational Model for Hybrid Observations with LCRD

There are currently no spacecraft deployed in an orbit around Earth with the primary objective being Hybrid Observations. To advance the CML of the operational model of future Hybrid Observatories, we performed an experiment with the LCRD payload onboard the STPSAT-6 spacecraft. The LCRD mission shares several similarities with proposed Hybrid Observatories: (1) a space based laser and (2) ground stations performing AO imaging from small aperture telescopes. The successful experiments conducted by the LCRD team demonstrates the feasibility of connecting ground telescopes with space assets. The question remains, can LCRD work with a large aperture ground telescope that performs high-quality science observations? To address this question, our team worked with the LCRD mission team and the W.M. Keck Observatory to simulate the operational model for hybrid observations.

Figure 3 presents the four elements of the experiment: (1) the LCRD laser payload, (2) the W. M. Keck Observatory, (3) the LCRD space operations team at NASA GSFC, and (4) the position of the laser source in the sky as seen from Maunakea. The LCRD payload holds two laser terminals, OST-1 and OST-2. During the experiment, either a single terminal or both will illuminate the Observatory with a known wavelength (1550 nm), power, and on-off timing sequence (i.e., knowledge of when the laser is activated or deactivated). With these parameters, our team can simulate each stage of the Operational Model of Hybrid Observatories. We provide a hierarchical breakdown of the LCRD-Keck experiment in Figure 4. The specific sequence of operations that were planned for this technical demonstration is provided in Table 2. In the following sections, we discuss each stage of the experiment. Specifically, we outline the work and preparation, as well as the results. In all cases, we demonstrate the promise of future hybrid observations.

Table 2: The Sequence of Operations for the Technical Demonstration with LCRD

Phase	Mission Time	Input	Output
Pre-Planning	-6 Months	Propose for Keck time	Awarded half of an engineering night
	-3 Months	Submit Proposal to point LCRD at Keck	Gain access to LCRD payload
	-1 Month	Receive Spacecraft TLEs	Create First Trajectory Prediction
Planning	-1 Week	Select non-LCRD targets	Create Observing schedule for night
	-5 Days	Meet with Ground Team	Establish Instrument Configuration
	-3 Days	Receive Updated Spacecraft TLEs	Create new Trajectory Prediction
Preparations	-12 Hours	Create list of 15th mag stars near LCRD position every 15 minutes	Enable the ability to calculate pointing offsets before tracking
	-5 Hours	Receive Final Spacecraft TLE file	Create Final predicted trajectory and submit starlist to telescope operator
	-1 Hour	Head to remote observing room at Keck HQ	Open communication lines with Space and Ground Teams
Execution	-30 Minutes	Confirm status of LCRD spacecraft	Point both OST-1 & OST-2 towards Maunakea
	-10 Minutes	Both OST-1 & OST-2 activate laser to 0.5 W	Illuminate Maunakea with a known illumination pattern
	0 Minutes	Telescope Operator slews to predicted location of Spacecraft	Identify spacecraft on Acquisition Camera from reflected sunlight & center target on NIRC2
	$+10$ Minutes	Begin capturing science frames of 1550 nm laser with NIRC2	Gather insights on how observing conditions effect LCRD flux
	$+20$ Minutes	Prepare AO system	Close the AO PyWFS loop on the LCRD laser source
	$+1$ Hour	Point OST-1 away from Maunakea	Analyze effects on LCRD flux and AO performance
	$+2$ Hours	Deactivate OST-1 & OST-2 & collect calibration frames for NIRC2	Transfer all spacecraft & telescope data to Observing PI

Fig 3: **Draft Image -khall** An illustration of the AO observation sequence. The LCRD's spacecraft is located on the STPSAT-6 spacecraft, on a geosynchronous orbit, 35000 km from Earth. The LCRD is moving with respect to the background sky at a rate of 15 arcsec/s. At the time of the observation the spacecraft will be located at 35.632°(el), 109.407°(az). The Keck II telescope is located at 19.8230°N, 155.4694°W and an altitude of 4225m. Top left: Illustration of the LCRD pointing its laser toward Keck Observatory. Bottom Left: Keck Observatory. Top Right: LCRD as seen from Keck for the observation. Bottom Right: GSFC LCRD Control Room.

3 Creating High Fidelity Tools to enable tracking and prediction of space-borne assets to be used by hybrid observatories

When we consider traditional observations performed with either ground or space-based observatories, one of the most basic objectives you must complete is a successful telescope pointing. Traditionally, an observer will utilize images from an acquisition camera from the ground and compare the image with an archived star chart to ensure correct telescope positioning. If one observes a sidereal target, no further corrections are normally required (excluding dithering). If an observer seeks to capture a non-sidereal target, such as Solar System targets, they will need to acquire its ephemeris. To do this, one requires accurate orbital information of the target to track its motion across the sky. Typically, Solar System targets have manageable angular rates (ΔRA & ΔDEC) for operators of large ground based telescopes to track with no issue. However, we must consider how this process will be impacted by the orbital configuration of the spacecraft hosting the LCRD payload.

The spacecraft is in a geosynchronous (GEO) orbit with an orbital radius of $\approx$ 35,000 km from Earth. From the perspective of an observer on the ground, the satellite will remain fixed at a constant Altitude and Azimuth (Alt & Az). As a result, the spacecraft will streak past background stars at a rate of 15 arcseconds per second. At a quick glance, this constant motion across the sky

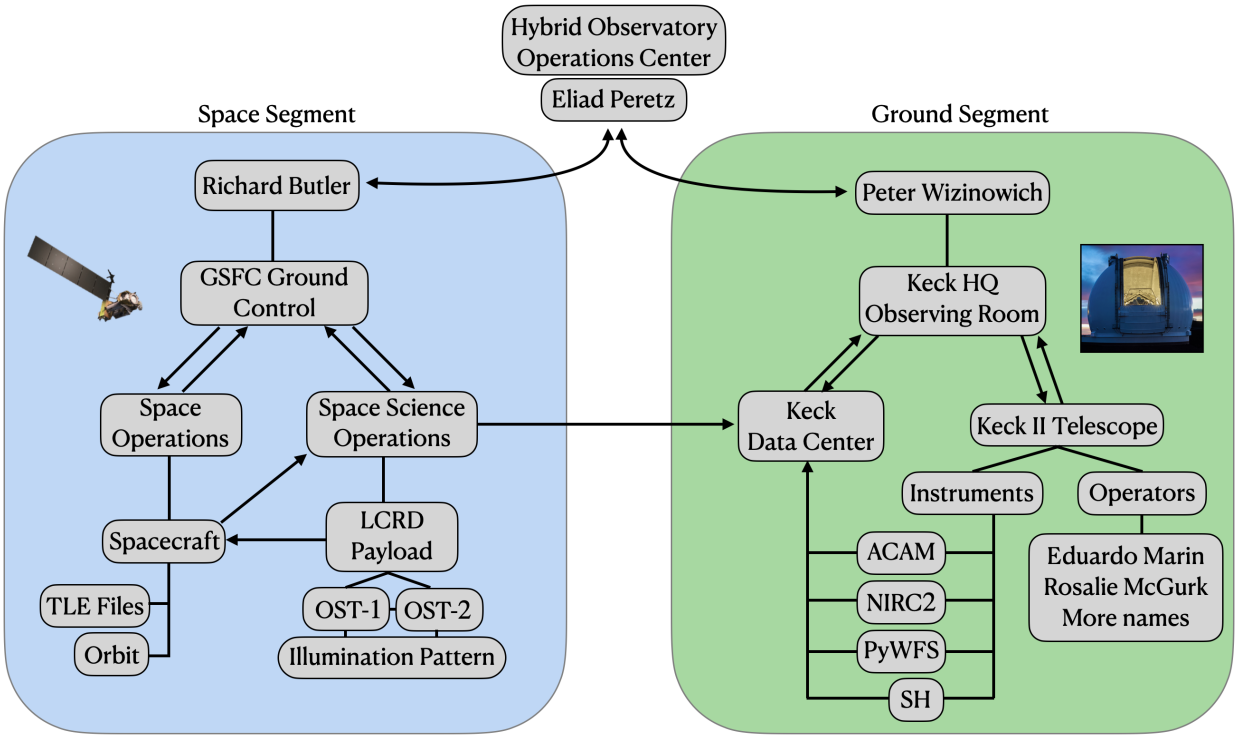

Fig 4: A hierarchical breakdown of the LCRD-Keck experiment.

should be manageable for the operator to lock-on to and track. In reality, the spacecraft will not remain at a fixed Alt and Az due to the imperfections of the spacecraft's orbit. The combination of its fast angular rate and its oscillatory motion of its position on the sky significantly complicates the planning and scheduling of the observation, as it may quickly drift from its previous position. To achieve our first goal, as outlined in Section 1.2, it is critical that we can reliably create a target list to keep the spacecraft in view throughout the observation to validate the operational model of the future Hybrid Observatories.

A common tool used by Solar System observers is the Horizons Ephemeris Service offered by the Solar System Dynamics (SSD) group at NASA's Jet Propulsion Laboratory. It is used to create star lists (i.e., coordinates) for planning observations of current large ground-based telescopes. To date, the program has not been used to schedule observations of an artificial satellite, especially one with an irregular motion across the sky. One can use the Horizons system by specifying your location on Earth and the orbit of the desired target to predict its location on the sky as a function of time. Two-Line Elements (TLEs) are a standard format for encoding a target's orbital parameters, such as the orbital inclination, right ascension of the ascending node, eccentricity, argument of perigee, mean anomaly, and mean motion. The Horizons Ephemeris service converts the orbital elements in the TLE into the satellite's position in the Earth-Centered Inertial (ECI) coordinate system. The ECI coordinates are then transformed into the Earth-Centered, Earth Fixed (ECEF) coordinate system, which accounts for Earth's rotation. Finally, the ECEF coordinates are converted to topocentric coordinates, which are relative to the sidereal time and the location of the observer on Earth (i.e., latitude, longitude, and altitude). From this process, we can predict both the Right Ascension and Declination (RA and DEC), and its apparent angular rate in both RA and

DEC (ΔRA and ΔDEC).

The LCRD mission team provided the ground team with TLEs three weeks in advance of the first night of the observations in January. Using the Horizons Ephemeris system, we specified the Keck Observatory during the hours allotted for the observation to create the first predicted trajectory of the spacecraft. Figure 5 presents the predicted trajectory, position in the sky, and the angular rates. There are inherent uncertainties nested within this technique. The specific orbital elements will exhibit alterations on time-scales of days. As a result, the flight team continually provided TLEs to the ground team to observe how the prediction evolved with time. We overlay all predictions together in Figure 5. This exercise was of specific importance as future Hybrid Observatories will need to have precise knowledge of the spacecraft's position, and we can inform the observational planning procedures for future missions. As seen in Figure 5, the final predicted trajectory a few hours before the first night of observations has significant differences when compared with the three week old prediction.

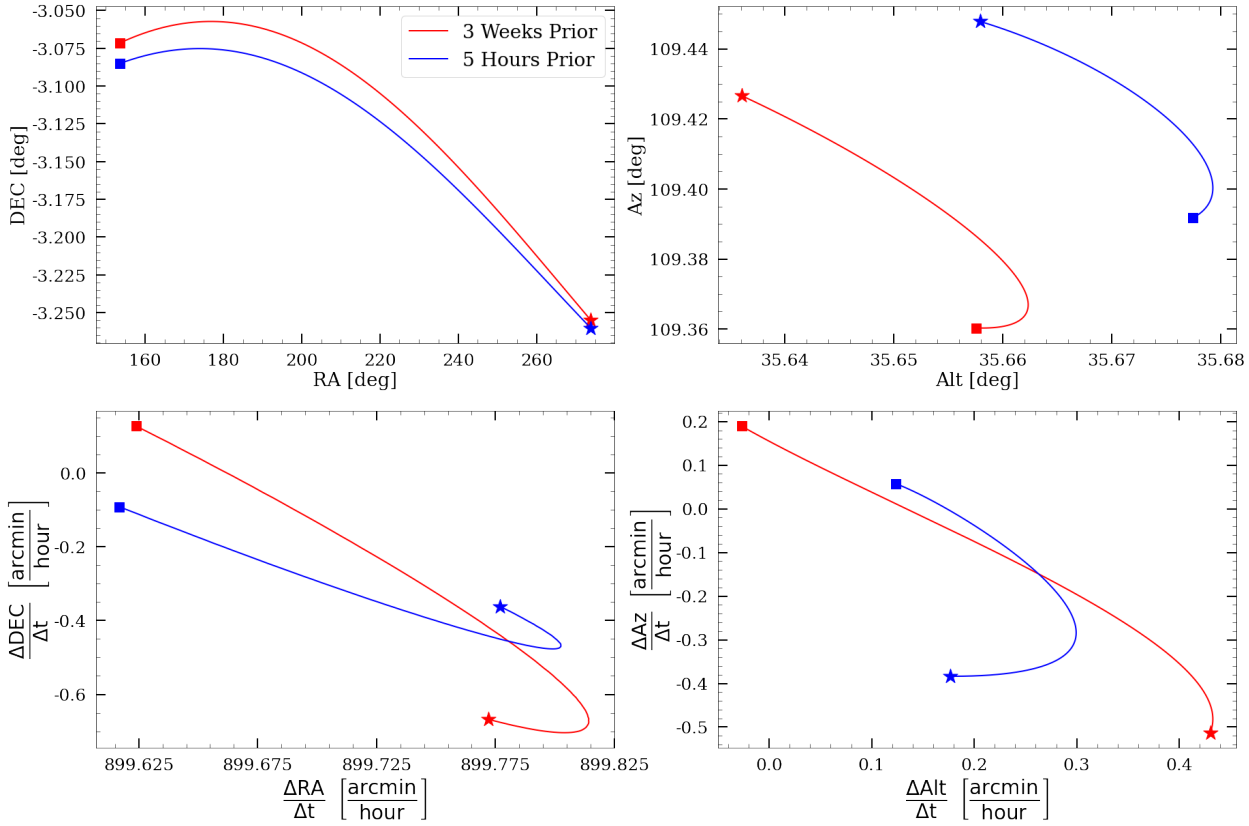

Fig 5: Predicted Trajectories of the LCRD spacecraft. *Top-Left*: The RA and DEC of the spacecraft, *Top-Right*: The Altitude and Azimuth, *Bottom-Left*: The change in RA and DEC as a function of time, *Bottom-Right*: The change in the Altitude and Azimuth as a function of time. In all panels, the prediction corresponds to 09:00-17:00 UT on the night of January 25 2024. The square and star correspond to the beginning and end of the trajectory respectively. Each prediction is labeled in the Top-Left panel.

Once the final coordinates were generated for the LCRD spacecraft, the ground team was ready

to perform observations. We used the Keck II telescope to image the 1550 nm laser source from both OST-1 and OST-2 onboard the spacecraft with both the wide and narrow-field modes of the NIRC2 camera. With both beacons activated and directed down onto the mountain, the spacecraft would be far too bright for NIRC2. To reduce the brightness, we used a variety of filter wheel combinations: the PK50_1.5 + CH4_short, PK50_1.5 + Hcont, and H + clear. We followed the following target acquisition procedure: (1) Identify the coordinates of the spacecraft's position at a future time and slew to a nearby 15th magnitude star to apply offsets, (2) slew to the predicted position of the spacecraft at the corresponding time and track with the angular rate of motion from the prediction, (3) search for the reflected sunlight from the spacecraft with the acquisition camera, (4) center the spacecraft on the NIRC2 detector and perform observations. During the first night of observations, we experienced heavy cloud cover and foggy conditions. In fact, Keck II was the only telescope still performing observations on the mountain during this night. There was a concern that these poor weather conditions would disrupt this procedure. However, breaks in the fog enabled successful spacecraft identification with the acquisition camera and NIRC2 imaging. Figure 6 presents the raw images captured of the laser source provided by both OST-1 and OST-2 pointed towards the mountain. Unfortunately, the first night of observations were cut short due to increased humidity and strong winds. During the second observing run in February, we had clear conditions making the spacecraft acquisition procedure much more efficient. While these results do not appear significant, they validate the Hybrid Observatory procedure model. Large ground based telescopes can indeed lock onto streaking satellites efficiently, opening up the door for future observations.

3.1 Performance of the Predicted Trajectories

While both observations were able to successfully image the spacecraft, we are now interested in the performance of the predicted trajectories. Specifically, how does the predicted trajectory from the TLE files compare with the trajectory measured by Keck? As discussed previously, the earlier predictions that were made weeks in advance of the observations possess significant offsets from the latest predictions. Before the comparison is made, we expect to find some offsets between the final prediction and the measured position of the spacecraft. Quantifying these offsets will enable key insights for the operational model of Hybrid Observatories.

To measure the trajectory of LCRD during both nights of the observation, we utilize the telescope pointing recorded in the header file of all raw science frames. We map a World Coordinate System (WCS) to each NIRC2 image to measure the position of the satellite within each frame. As one can see in Figure 6, the spacecraft drifts from the center of the frame, so we cannot rely on the telescope pointing alone. When mapping the WCS onto each image, we apply the distortion corrections for both the wide and narrow camera. We should note that the laser payload is the only source in all raw frames. As a result, we cannot improve the WCS solution by locating known background stars streaking through the FOV. In Figure 7, we compare the predicted trajectory of the satellite from the TLEs against the measured value from NIRC2. We find a consistent offset between the measured and predicted value during both nights. While these offsets appear severe, we stress that little time was required to acquire the satellite and begin imaging with NIRC2.

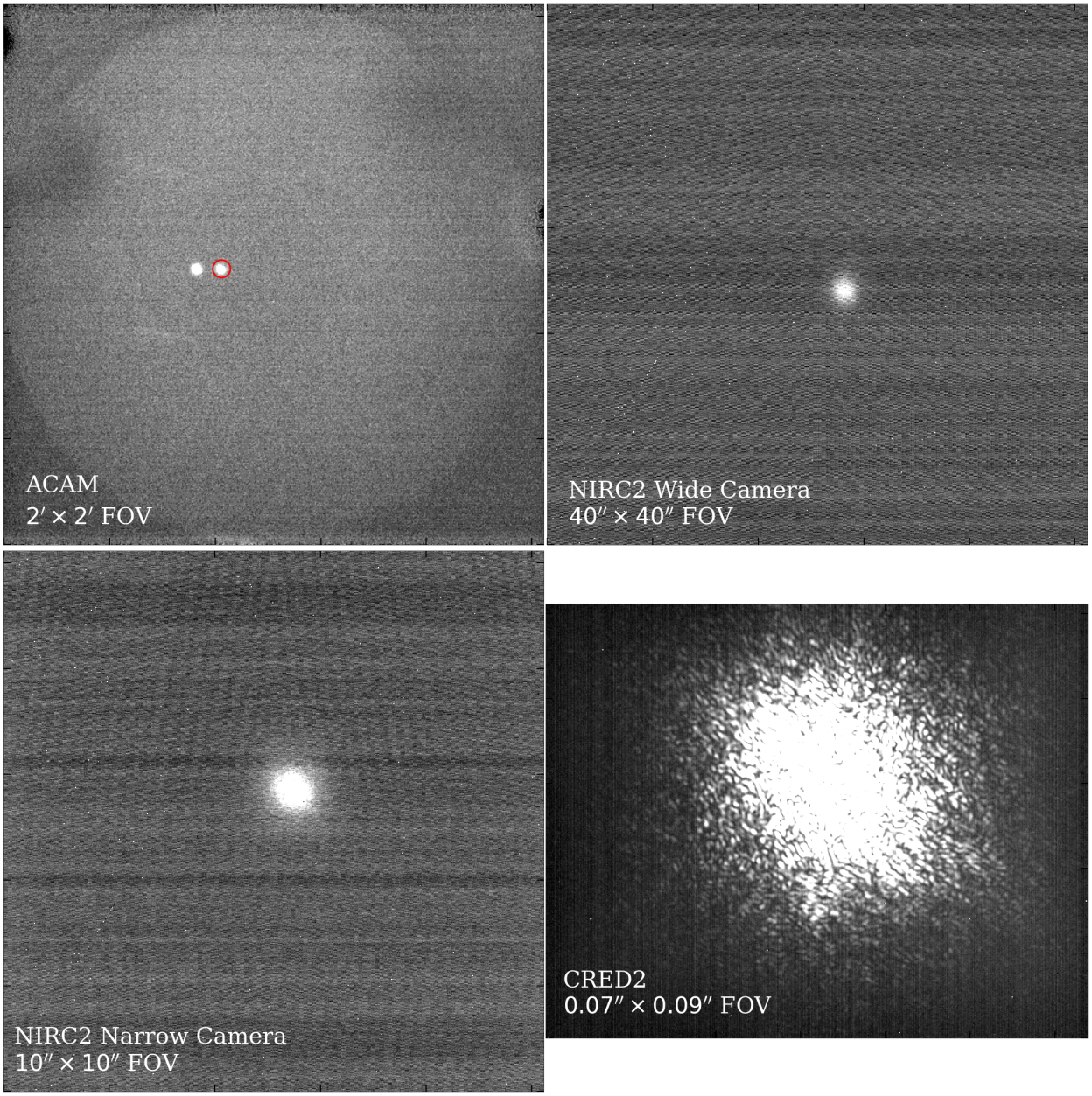

Fig 6: Raw images of the laser source from LCRD. *Top-Left*: The view of LCRD through the Acquisition camera (ACAM). The red circle marks the satellite position (the image to the left is a ghost reflection from the second surface of a beamsplitter). *Top-Right*: The NIRC2 wide-field camera image of the laser source. *Bottom-Left*: Same as the top-right panel, but with the narrow-field camera. *Bottom-Right*: The LCRD laser source imaged with the CRED2 near-infrared imager.

As mentioned previously, the LCRD mission team provided the location of the spacecraft in ECEF coordinates as a function of time during the February 21st observing run. This provides us with a second comparison with the predicted trajectory by converting these coordinates into a topocentric RA and DEC. We present this comparison in Figure 8. There are two immediate conclusions: (1) The predicted TLE trajectory shares equal angular rates as the GPS position, and (2) there is a significant offset in the RA position ($\sim 400''$). It is unclear

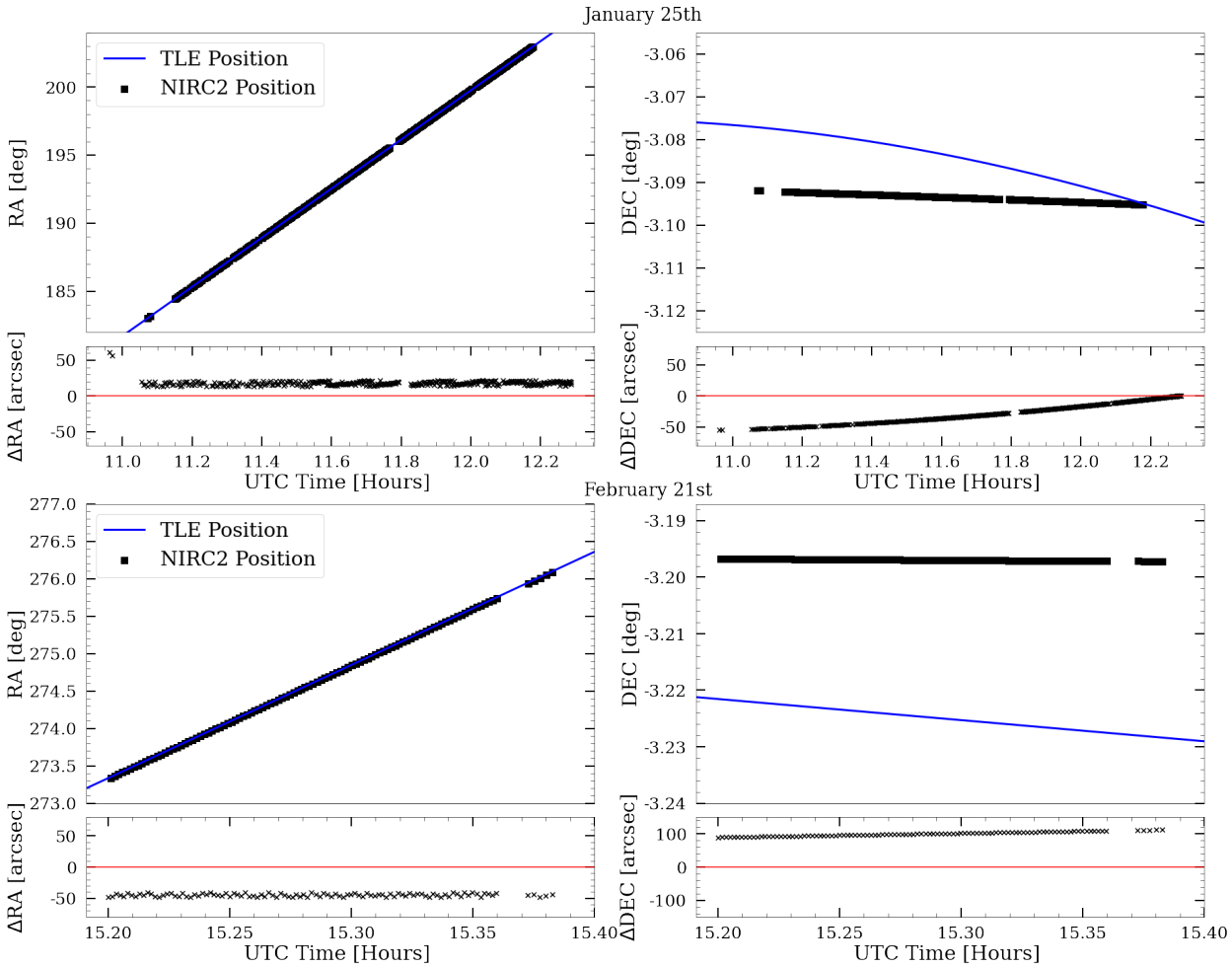

Fig 7: A comparison between the predicted and measured trajectory. The top and bottom panel corresponds to the January and February observations, respectively. *Left*: The RA as measured by NIRC2 as a function of time as black dots. We overlay the predicted trajectory from the TLE file in blue. *Right*: The NIRC2 DEC as a function of time versus the TLE file.

Through the successful acquisition and tracking of the LCRD spacecraft, we have demonstrated the viability of future Hybrid Observatories. Despite its apparent simplicity, the capability of a large ground-based telescope to effectively collaborate with an orbiting spacecraft was uncertain. The results presented herein enhance both the CML and TRL of Hybrid Observatory operational models. This was only the first phase of the technology demonstration. We now transition onto the next objective, closed-loop AO imaging.

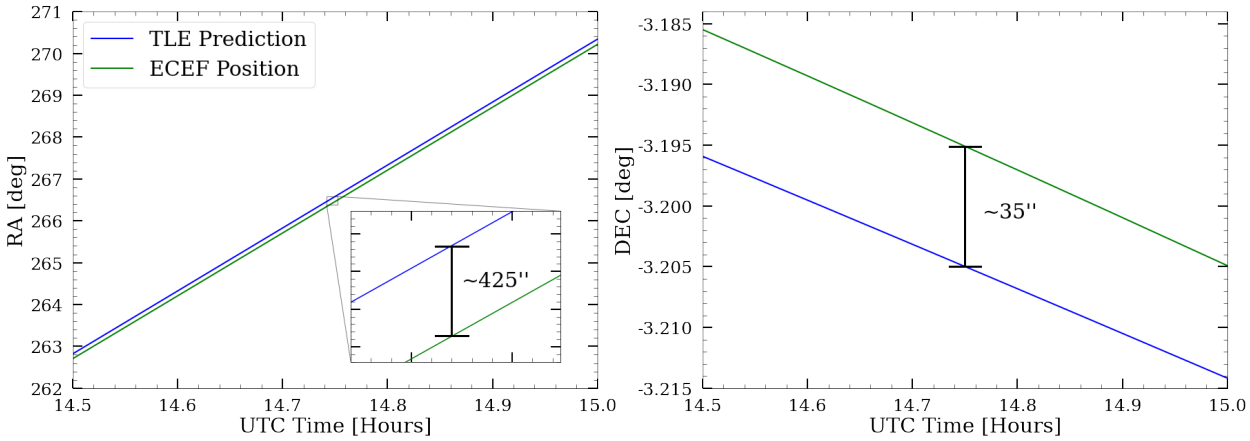

Fig 8: A comparison between the TLE trajectory and the position of the LCRD payload. In blue, we plot the TLE trajectory as seen in the bottom panel of Figure 7, and we plot the spacecraft's position, as measured by the spacecraft team, in green.

4 Closed-Loop AO Imaging with LCRD

Into - Motivation*

We have demonstrated that large ground based telescopes can lock onto and track geo-stationary satellites. However, simply taking images of a laser source from the ground does warrant future investment and effort by itself. Once we lock onto the satellite, we must demonstrate that closed-loop AO imaging is possible. The ability to adjust the location of an artificial star to perform high resolution AO imaging will push the boundaries within several scientific fields. In this section, we discuss our attempt at closing the loop with the laser source onboard the LCRD payload.

To perform closed-loop AO imaging with NIRC2, we incorporated both the Pyramid Wavefront Sensor (PyWFS) and the Shack-Hartmann Wavefront Sensor (SHWFS). Both of these are standard tools used to significantly enhance near-IR observations from the ground. Typically, observers will utilize a sidereal target (i.e., a star) to close the loop, unless a Solar System object is selected (tag the asteroid experiment). For this experiment, we must close the loop on a target that is streaking at 15 arcseconds per second, and as we show in the previous section, it will continuously drift within the field. Additionally, stars do not experience dramatic variations in their observed flux on short time scales (e.g., fractions of a second). The laser source from LCRD does not act like a true star; the observed flux from the ground is highly variable due to beam pointing instability, as we will discuss in Section 5. The LCRD normally receives an uplink beacon from its ground stations to reduce the jitter in the beam. Despite these limitations, we attempted to close the loop during both nights.

On the first night of observations in January, the combination of beam instabilities and cloud obscuration restricted our ability to close the loop on the satellite. Right before the weather required the dome to be closed, we nearly closed the Tip-Tilt loop with LCRD before the flux dropped due to heavy cloud cover. As we will discuss later, the clouds had a significant impact on the measured flux from the laser source. For the remainder of this section, we will focus on the results from the February observation, as we had much more favorable weather.

We began the February observation with the SHWFS to perform closed-loop AO on reflected sunlight from the LCRD satellite while imaging with the NIRC2 wide-field camera. Our filter wheel combination was PK50_1.5 + CH4_short. To begin the night, the LCRD team directed both OST-1 and OST-2 onto the mountain. With both terminals pointed at Keck, the flux from the spacecraft remained more stable. Additionally, we experienced no cloud cover that could have obscured the source from the detector. However, we should note that the laser source still experienced variability, which we will discuss in detail in Section 5. We successfully closed the AO loops with the SHWFS near the beginning of the night, shortly after acquiring the spacecraft. The middle panel in Figure 9 presents the high resolution NIRC2 image of the LCRD laser source. The FWHM of the PSF from the laser source was X mas. Once we were satisfied with the images collected, we switched the AO configuration to the PyWFS. As before, both OST-1 and OST-2 onboard LCRD were shining down onto the summit. As shown in the right panel of 9, we successfully closed the loop on the PyWFS to achieve a FWHM of X mas.

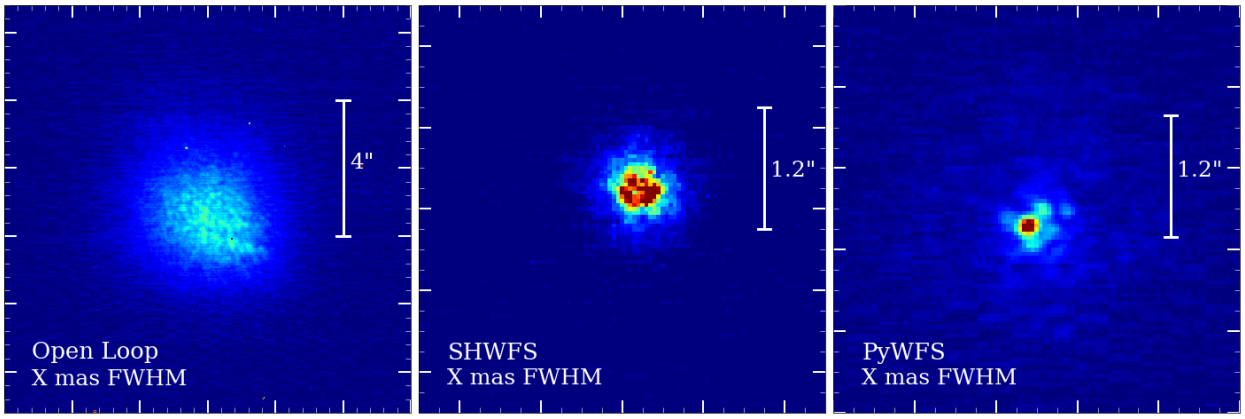

Fig 9: High resolution NIRC2 images of the LCRD laser source. *Left*: Open loop image. *Middle*: AO corrected image after closing the AO loop on reflected sunlight from the satellite with the SHWFS. *Right*: AO corrected image after closing the AO loop on the LCRD laser with the PyWFS. For the AO corrected images, we zoom in on the laser source for clarity and provide a scale bar to note the difference in scale. The FWHM of each PSF is marked in the bottom left corner of each panel.

Closing the loop on the LCRD laser source signifies a major achievement. The results presented here push forward both the CML and TRL of the Hybrid Observatory operational model. We stress that the LCRD mission was not optimized to perform collaborative observations with large ground based observatories such as Keck. Specifically, its orbit does not enable access to science targets one expects to study through high resolution AO imaging. Future missions that combine space-borne lasers and ground telescopes will be able to leverage this improved AO-corrected image quality, and this experiment has validated this approach.

The remaining question we are left with is how stable of a source is required to close the loop, as it has the chance to significantly impact the feasibility of AO imaging. As we discussed previously, the heavy cloud and fog cover restricted us from closing the loop on the satellite. Once we were satisfied with the results using both the SHWFS and PyWFS on both OST-1 and OST-2

pointed towards Keck, we chose to deactivate OST-1. With a single laser pointed down towards the mountain, the pointing beam instability worsened, as both beams would reduce the overall jitter due to averaging. Interestingly, we began to have issues closing the loop with the PyWFS. Again, we note that Keck did not transmit a beacon towards LCRD to improve the pointing accuracy. This will need to be in consideration during the planning stages of future observations with Hybrid Observatories.

5 Lessons for Future Flux- Calibration missions

So far, we have demonstrated the feasibility of future Hybrid Observatories by accomplishing the goals and objectives listed in Table 1. As discussed previously, one of the primary science goals of future Hybrid Observatories is to perform flux calibration, and the LCRD provided an ideal laboratory for the ground team to perform tests. The final question yet to be answered is the ability to perform flux calibration using a space-borne laser from the ground. This scientific payoff alone can justify future investment into this effort. The calibrated laser beam will traverse the same path through the earth's atmosphere, telescope and instrument (for example wavefront corrections) as the target stars - and this will reduce the flux calibration uncertainty measured for the target star. However, due to problems of weather discussed above we did not observe background standard stars. Here we show the measurement of the flux from the laser terminal. Let's begin with operations performed by both the ground and space teams. The LCRD team powered both OST-1 and OST-2 to 0.5 W. If we first imagine an ideal scenario, there would be no atmosphere and the beam would point directly down the center of the telescope aperture. The ground team can simply calculate the expected count rate from both OST-1 and OST-2 by assuming a Gaussian beam with a known divergence. In reality, the situation is much more complicated due to the beam pointing instability. As discussed in the previous section, the LCRD payload typically locks onto a transmitted beam from the receiving station to reduce the instability. This was not possible for the observations with Keck II. As a result, the beams from both laser sources varied on the ground as a function of time (Fig 10, a cartoon that illustrates the beam pointing instability on the ground). To quantify how this instability impacts our ability to perform Flux Calibration, we sampled a variety of exposure times. To motivate this, we need to understand how the exposure time could impact the expected flux from the laser source.

The raw data is received using FITS files with each file containing 62 separate layers of information, 152x128 pixel subarray, and being analyzed using a customized python notebook photometry tools design for NIRC2 data reduction process. First we correct the data by removing the dark, dividing by the flat field, and subtracting the background. Each corresponding master dark frame was subtracted from all science frames. At the end of the February observation night, we attempted to obtain flat field images with a flat field lamp on, however, the lamp failed. As a result, we downloaded the lamp-on flat frames for the CH_4 filter taken on June 9th, 2023 from the Keck Observatory Archive (KOA)[1]. For any frame where the subarray was used, we simply extracted the 152×128 region from the archived data. Finally, we performed simple sky subtraction by producing median-combined master sky frames when the LCRD was not in view. The method involves similarities to 3D IFU "optimal extraction" codes, but the reduction to 2D simplifies the process. For each frame, we generated a Signal-to-Noise (S/N) map by estimating the Root-Mean-Square (RMS) of each reduced science frame. From there, we mask all pixels with a $S/N < 4$. Next, we locate pixels that are clustered together. The algorithm will assign an ID to each group. We mask all groups that have fewer than 10 pixels. In this way, we remove any "floating islands" from the field which correspond to any remaining artifacts. Then the centroid of the target was found using DAOStarFinder, which finds the X and Y values of the pixel with the maximum counts. Finally, we recover the counts rate by simply adding up all count within the final aperture and dividing

[1] https://koa.ipac.caltech.edu/cgi-bin/KOA/nph-KOAlogin

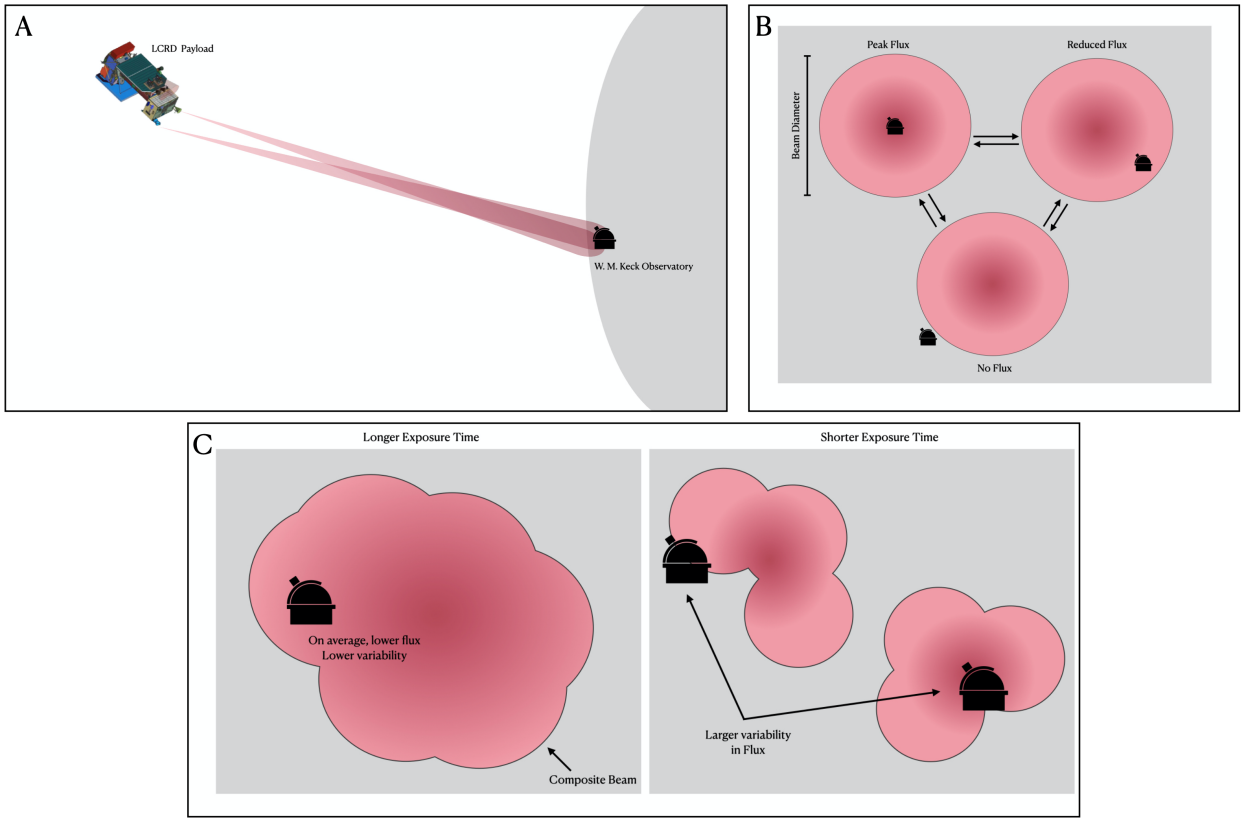

Fig 10: Diagram that illustrates the expected flux variability from the LCRD payload. All diagrams are not to scale. *Panel A*: The LCRD spacecraft in its GEO orbit at $\sim$ 35,000 km pointing both terminals at Keck. *Panel B*: A cartoon demonstrating how the beam instability effects the measured flux. Each circle corresponds to the beam from a single laser source, and the telescope refers to Keck-II. NIRC2 will record the highest flux values near the center of beam and little to no flux near the wings of the beam. *Panel C*: An illustration of how the exposure time can impact the flux. Longer Exposure times will allow the varying beam to smear across a larger area, creating a semi-stable flux. However, the shorter exposure has an increased chance to sample different regions of the beam, which will increase the variability.

by the total exposure. Essentially, it builds a customized aperture for any given image, after the regular reduction steps have been performed.

In order to get the magnitude from the counts rate we need to use the magnitude zero point of the filter. The magnitude zero point is the magnitude of an object that produces 1 count/sec on the detector. This can be calculated by: $m0 = m1 + 2.5log10(F1)$, where m1 = the magnitude of a target from a known measurement (catalog), and F1 = the flux of the target. However, $'CH4short+PK501.5'$ has no recorded photometric zero point and therefore we can not need to calculate the specific magnitude zero point to get the magnitude of the LCRD collected using NIRC2.

Figure: different WL /counts of flux - ACAM and CRED2 and NIRC2.

Simulating the expected count rate of LCRD to compare with the flux estimates was done using an estimation of a dovrtence of the beam size, as well as the pointing error so we are unlikely to see the center of the beam. When comparing, we can see that the estimated count rate is mostly relay in the same location as the calculated counts rate. As described in Figure 10, we can see that even

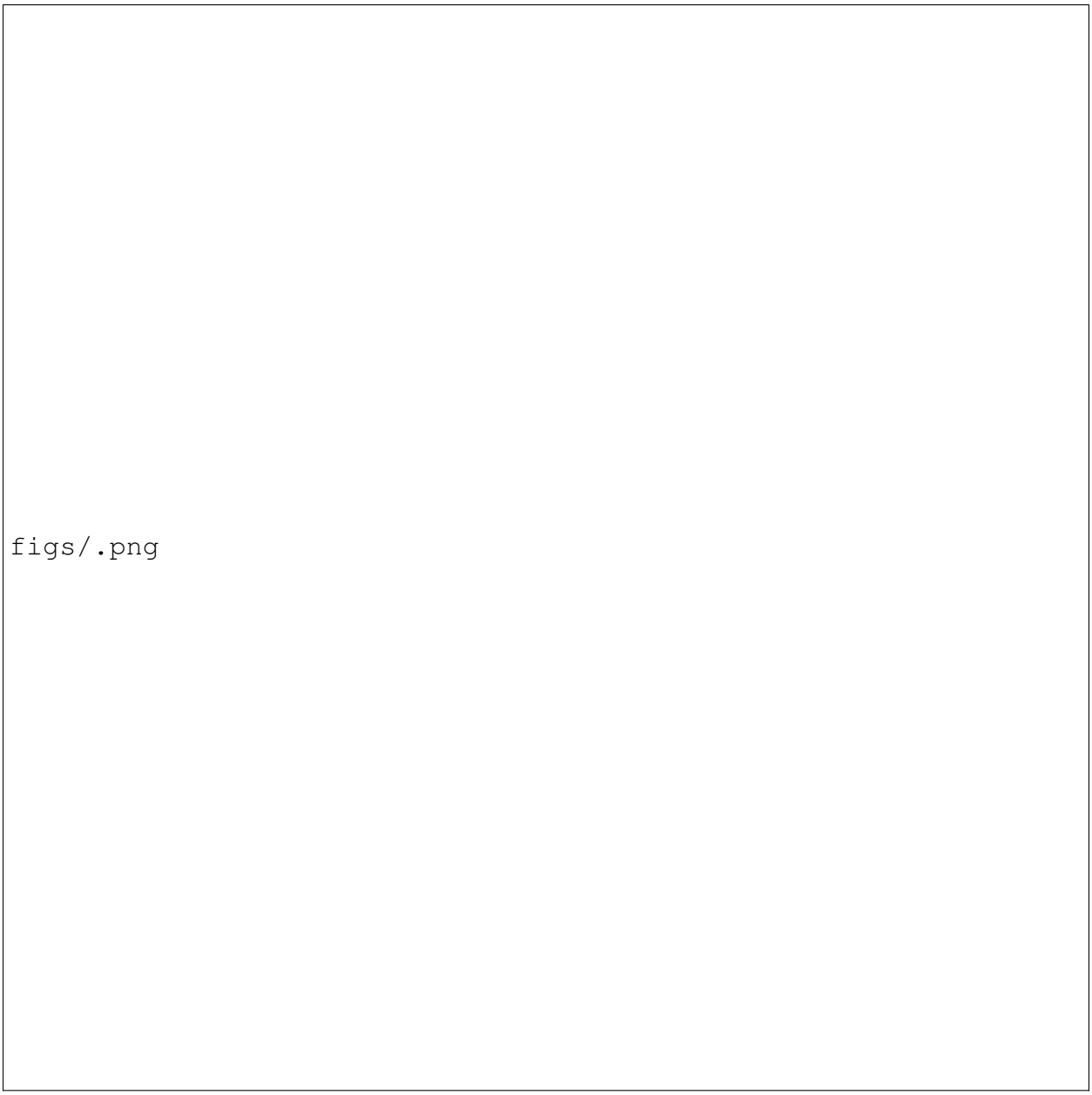

Fig 11: raw data, and how we subtract the data: raw, dark, flat, (Raw-dark)/flat

with the same exposure time, there is a large variation in the count rate data. There is a clear trend of decreasing count-rate with the time of the experiment. We can see three different segments of the observing time based on the exposure time and coadds. . From figure 13 we can see that the counts rate using the CRED2 is around 4-7 orders of magnitude larger then the ones using NIRC2. There are fewer frames available for CRED2, and they have different exposures than the NIRC2 images.

-Background noise at different WL? the brightness of the source - compare with the measured flux rate

What we need in order to try and get the flux: Acquire image: using filter with 0 point magnitude (during this experiment we did not use a filter with ZPM For NIRC-II, FILTER =

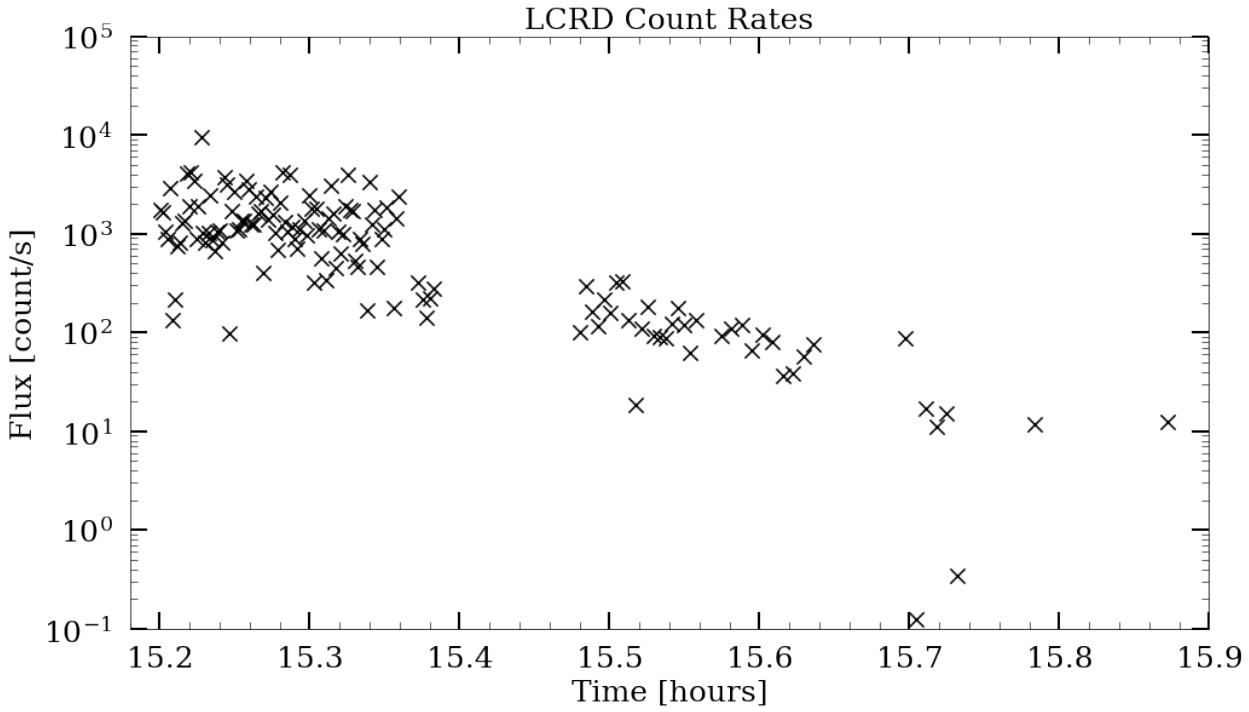

Fig 12: NIRC2: LCRD count rate vs time, measured flux vs estimated lcrd flux

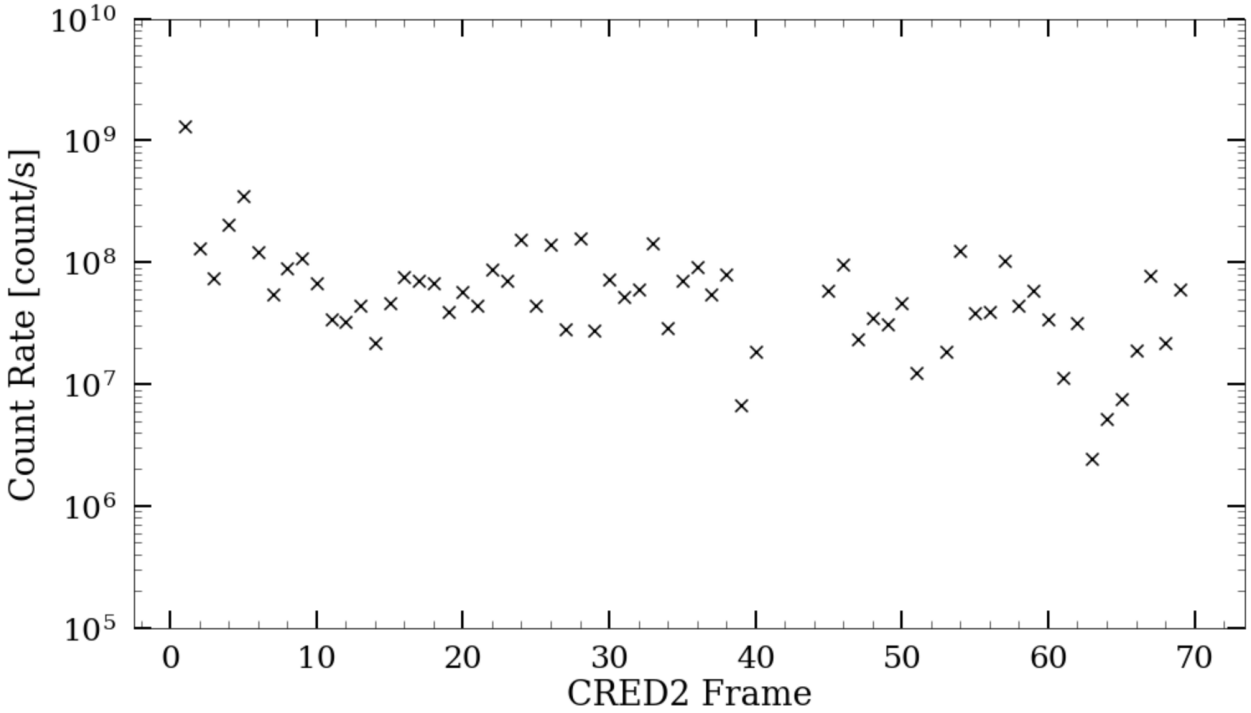

Fig 13: different WL /counts of flux - ACAM and CRED2 and NIRC2.

'CH4$_s hort + PK50_1.5'$).

Turn on the OST1 and OST2 of the LCRD (the two terminals should be on): Moreover, When the two laser terminals, OST-1 and OST-2 are turned on it was possible to observe the laser beam.

However, when one of the OST was turned off, the telescope could not find the laser source, and collect the data. This means that the two OSTs should be turn on to be able to do hybrid observatories and specifically flux measurement.

Also use close loop pointing because the signal is not stable.

Shorter exposure time: It appears that there is less dispersion within the middle zone, and that when the exposure time is shorter, the count rate is higher. It make sense that the faster the exposure time is, there is more chance to catch the peak of the laser, and get higher count rates. We recommend to collect the data with the shorter possible exposure time.

Get the fits files, and create the background images: flat (During this experiment we used catalog file due to technical problems), dark, sky/ images of the LCRD with the lasers off (OST1 and OST2 off). Create bad pixels map to remove and ignore the inaccurate pixels.

Reduce the data from pixel to pixel variation (flat) and thermal excitation (dark): -Darkfield (D), (D), -Subtract the background.

Find the centroid of the target to locate the source using DAO starfinder.

Create circular apertures with different radii around the centroid of the target and compute the sum of the pixel values within the apertures, and the count rate.

Calculate the flux and the magnitude.The magnitude of an object (per filter and wavelength): m1=-2.5log(f1)+m0

...

6 Discussion and Conclusion

Acknowledgments

This unnumbered section is used to identify those who have aided the authors in understanding or accomplishing the work presented and to acknowledge sources of funding.

References

1 Astropy Collaboration, A. M. Price-Whelan, B. M. Sipőcz, et al., "The Astropy Project: Building an Open-science Project and Status of the v2.0 Core Package," **156**, 123 (2018).

2 Astropy Collaboration, A. M. Price-Whelan, P. L. Lim, et al., "The Astropy Project: Sustaining and Growing a Community-oriented Open-source Project and the Latest Major Release (v5.0) of the Core Package," **935**, 167 (2022).

The authors wish to recognize and acknowledge the very significant cultural role and reverence that the summit of Mauna Kea has always had within the indigenous Hawaiian community. We are most fortunate to have the opportunity to conduct observations from this mountain.

This work made use of Astropy:[2] a community-developed core Python package and an ecosystem of tools and resources for astronomy.[?,1,2]

List of Figures

[2] http://www.astropy.org

List of Tables